JOURNAL OF MATERIALS SCIENCE **40** (2005) 605–608

# Mapping and analysis of microscopic Seebeck coefficient distribution

H. L. NI, X. B. ZHAO*
*State Key Laboratory of Silicon Materials, Zhejiang University, 310027 Hangzhou, People's Republic of China*
*E-mail: zhaoxb@zju.edu.cn*

G. KARPINSKI, E. MÜLLER
*Institute of Materials Research, German Aerospace Center (DLR), D-51170 Cologne, Germany*

Understanding the local Seebeck coefficient distribution is helpful for the development of novel thermoelectric materials. Seebeck coefficient distributions of both zone melted and hot pressed samples of I-doped $Bi_2Te_3$ based alloys were measured using microscopic Seebeck coefficient mapping method. Seebeck coefficient differences up to 40–50 $\mu$V/K were found between different locations on the same sample. There is no visible relationship between the microscopic Seebeck coefficient distribution and the local surface morphology and element distributions. It is suggested that the local Seebeck coefficient variations were mainly originated from the lattice defects for the zone melted sample and also due to the grain orientation for the hot pressed sample.


## 1. Introduction

Thermoelectric materials can be used to convert heat directly to electricity for power generators, or reversely in refrigeration devices [1, 2]. Thermoelectric devices have many advantages such as no moving parts, no pollution, no noise and free from maintenance. Novel compounds and nanostructured materials have been of interest recently and intensively investigated [3–8]. The property of a thermoelectric material is characterized with the figure of merit, $Z = \alpha^2\sigma/\kappa$, where $\alpha$ is the Seebeck coefficient, $\sigma$ is the electrical conductivity and $\kappa$ is the thermal conductivity. Among them $\alpha$ is the most significant parameter since $Z$ is proportional to the square of $\alpha$. The Seebeck coefficient of a material is related with the transport properties of the carriers in the material, and originated from the electronic structure and scattering mechanism. In the view of materials science, Seebeck coefficient is considered to be a function of the crystal structure, chemical compositions and the microstructure features of the material, and treated experimentally as a macroscopic property obtained generally by measuring the thermoelectric potential and temperature difference between both ends of the sample.

The problem which here raises is that a microscopically homogeneous material has to be assumed in order to give a comprehensive understanding between the measured macroscopic Seebeck coefficients and the microscopic intrinsic features of the material. Recently, Shin *et al*. reported the measurements of Seebeck coefficients on nanometer scale [9], and found that the local Seebeck coefficients varies significantly in the sample. But they measured only along a 200 nm line. Svechnikova *et al*. [10] and Platzek *et al*. [11] have mapped Seebeck coefficients over large areas of Czochralski grown $SbI_3$ doped $Bi_2Te_{2.85}Se_{0.15}$ single crystals. A spread of about 30 $\mu$V/K has been measured on the surfaces perpendicular to the crystallographic $C$-axis. Here we report the mapping of microscopic Seebeck coefficients in $2 \times 2$ mm areas of two iodine doped $Bi_2Te_3$ based alloy samples prepared by zone melting and hot pressing, respectively, and discussed the measurements with the local surface morphology and element distributions over the same areas.

## 2. Experimental

Two samples of I doped $Bi_2Te_3$ based thermoelectric materials were measured in the present work. Both samples are about 2 mm in height and more than 5 mm in length and width. Sample A is cut from a zone melting directionally solidified ingot. The measuring surface is parallel to the solidification direction. Sample B is a hot pressed sample. The powder for sample B was milled from the material cut from the same ingot as sample A and passed through a sieve of 0.1 mm mesh. The hot pressing temperature, pressure and time are 350°C,

*Author to whom all correspondence should be addressed.

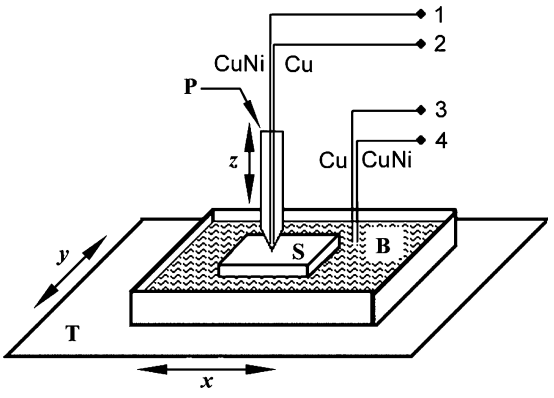


*Figure 1* Schematic drawing of the Seebeck Micro-Thermoprobe (P: micro-thermoprobe, S: sample, B: thermostat bed, T: position table).

50 MPa and 30 min, respectively. The measuring surface of sample B is vertical to the hot pressing direction. XRD analysis showed that both samples are single phase of $Bi_2Te_3$ ($R\bar{3}$ m). The samples were polished before the microscopic Seebeck coefficient measurement. The surface morphology of the mapping zone was observed after the measurement on a FEI-Sirion field emission scanning electron scope (FESEM). The distributions of elements were analyzed by an energy dispersive spectroscopy (EDS) attached on the FESEM. The mapping surface became rough after the microscopic Seebeck coefficient measurement due to the contact by the micro measuring probe. A small dent was marked at the upper right corner outside the mapping zone, so that the FESEM image can be exactly located with respect to the Seebeck coefficient mapping on the same zone.

The microscopic Seebeck coefficient distribution was measured in the Institute of Materials Research of German Aerospace Center (DLR) on a Seebeck Micro-Thermoprobe. Fig.1 illustrates the principle of the device [11]. The sample (S) is fixed on a thermostat bed (B) with a constant temperature on a position table (T). A heating micro probe (P), which can move down and up, heats the local on the sample surface where the probe tip contacts the sample, producing a temperature difference of about 3°C between the measuring point and the sample. Two thermocouples (Cu-CuNi) in the micro probe and the thermostat bed measure the temperatures of the measuring point and the sample, respectively. The Seebeck coefficient is calculated by $\alpha = U_{23}/\Delta T + \alpha_{Cu}$, where $U_{23}$ is the voltage measured between both Cu wires of the thermocouples, $\Delta T = T_{Tip} - T_{Sample}$ is the temperature difference between $T_{Tip}$, the temperature at the point contacted with the probe tip, and $T_{Sample}$, the sample temperature, and $\alpha_{Cu}$ is the Seebeck coefficient of metal copper. The device is fully controlled by computer and has a resolution of 10 $\mu$m, a point accuracy of 1 $\mu$m and a maximal random deviation on $\alpha$ of 2 $\mu$V/K.

## 3. Results and discussions

During the measurement the WC micro-thermostat pressed into the polished surface, leading to the local brittle destruction and producing the surface morphology as shown in Fig. 2a for sample A. This means that the surface morphology should reflect the local mechanical properties originated from the crystal orientations, grain boundaries, crystal defects and possible impurity precipitates. The measuring surface of sample A can be considered vertical to the $C$-axis of the $Bi_2Te_3$ lattice, since the solidification direction, arrow SD in Fig. 2a, should be vertical to the $C$-axis for the zone melted $Bi_2Te_3$ ingot. The measuring area (2 × 2 mm) would cover only a few grains for the slowly solidified $Bi_2Te_3$ ingot. A possible grain boundary is indicated with the small arrow GB in Fig. 2a. The Seebeck coefficient distribution of sample A is mapped in Fig. 2b. A difference on $\alpha$ values of about 40 $\mu$V/K can be measured in Fig. 2b according to the $\alpha$-scale. Some obvious features can be found in the $\alpha$-map, Fig. 2b. These are the broad light grey stripes (low-$\alpha$ zones) nearly parallel to the solidification direction, fine periodic stripes nearly vertical to the solidification direction (SD), and a discontinuous horizontal dark zone in the low-middle of the map (high-$\alpha$ zone). These features in the $\alpha$-map, however, do not remarkably correspond with the morphological features in Fig. 2a. Also the possible grain boundary, indicated as GB in Fig. 2a, seems to be of little influence on the local Seebeck coefficients.

The rectangle area in the right bottom of Fig. 2 were analyzed by EDS for the distributions of Bi, Te, Se and I. The results are given in Fig. 3. Some locations in Fig. 3 with low element contents are possibly due to the influence of the surface roughness on the EDS results. No remarkable relationship between the elements

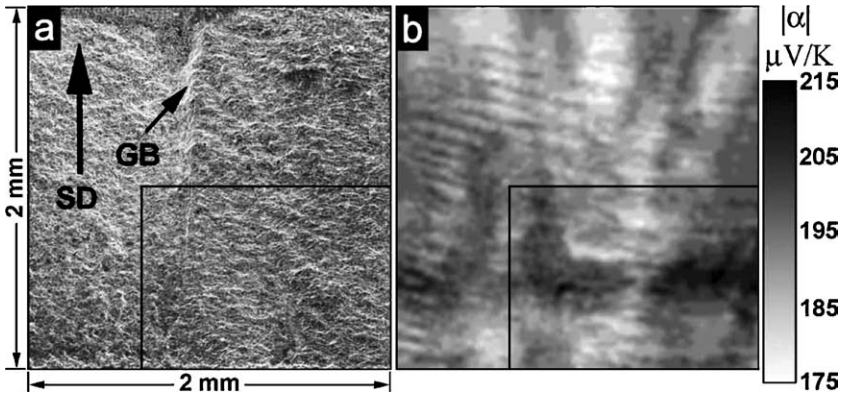


*Figure 2* The morphology (a) and Seebeck coefficient distribution (b) on the plane parallel to the solidified direction of sample A.

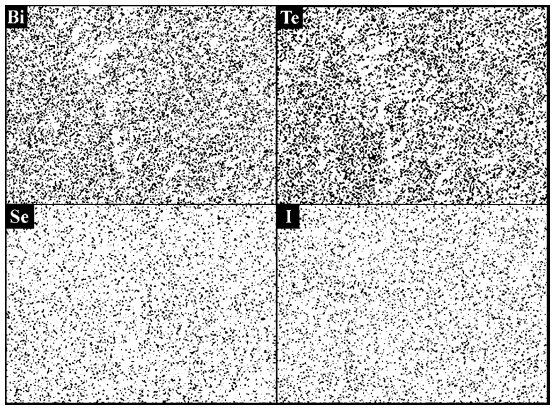


*Figure 3* Elements distribution measured by EDS in the right bottom rectangle of Fig. 2.

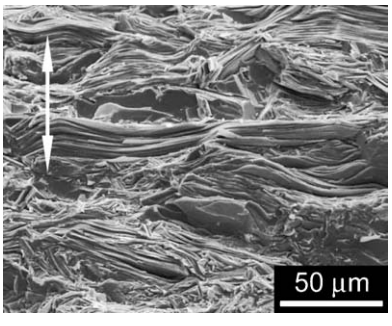


*Figure 4* SEM image of the hot pressed sample. The white arrow is the pressing direction.

distribution and the Seebeck coefficient distribution could be found, although a large Seebeck coefficient difference up to about 40 $\mu$V/K exists in the area.

In the hot pressed sample, the $C$-axis of crystals tends to be parallel to the hot pressing direction, as indicated by the morphology of sample B in Fig. 4. This means that the measuring surface of sample B, which is vertical to the hot pressing direction, should be vertical also to the $C$-axis. Fig. 5 shows the morphology and Seebeck coefficient distribution of Sample B. Fig. 6 shows elements distributions corresponding to the left bottom rectangle area of the sample. Also for the hot pressed some, no relationship between the Seebeck coefficient distribution and the morphology could be found.

Seebeck coefficient is a material property related to carrier transport. Both chemical feature, such as composition and doping, and microstructural feature, such as textures and crystal defects, have influences on the Seebeck coefficient of a material. Many theoretical and experimental investigations have been done for these influences on Seebeck coefficients. However, it was practically assumed that materials were homogeneous, since a Seebeck coefficient was generally measured under a temperature gradient across the whole sample. The local Seebeck coefficients measured in the present work are also the integrated effects of electronic structures in the local half-sphere zone with a temperature gradient from $T_{\mathrm{Tip}}$ at the probe tip to $T_{\mathrm{Sample}}$ of the sample. Considering the fact that the largest temperature gradient should occur near the point contacted with the probe tip, the local Seebeck coefficients measured in the present work could be considered as the result of the local carry transport in the corresponding half-sphere zone with a size of about a few micrometers. The grain sizes of both samples used in the present work are significantly larger than the micro-sized half-sphere zones. The results given in Figs 2 and 3 reveal that the local Seebeck coefficients could be very different even in a grain with the same crystal orientation and homogeneous composition distributions. The variations on the local Seebeck coefficients of the samples should be, therefore, originated from the possible crystal defects such as dislocations and stacking faults. Although this conclusion should be confirmed by further detailed investigations such as TEM observations of dislocations and stacking faults, the measurements of Svechnikova *et al.* [10] and Platzek *et al.* [11] on Czochralski grown single crystals and the our results on both zone melted and hot pressed samples support the conclusion. The density of possible crystal defects should be low for a single crystal and very high for a hot pressed sample, which is coincident with the measured Seebeck coefficient fluctuations of about 30 $\mu$V/K for the single crystals, 40 $\mu$V/K for the zone melted sample and near 50 $\mu$V/K for the hot pressed sample. The fine periodic stripes on the $\alpha$-map of the zone melted sample in Fig. 2b have a period of about 0.1 mm along SD. They are suggested to be caused by the periodic disturbance of external periodic fields or the mechanical vibration of the solidification device during the solidification of the material. The variation of the local Seebeck coefficients in the hot pressed sample should come from the different crystal orientations, since $Bi_2Te_3$ based alloys are

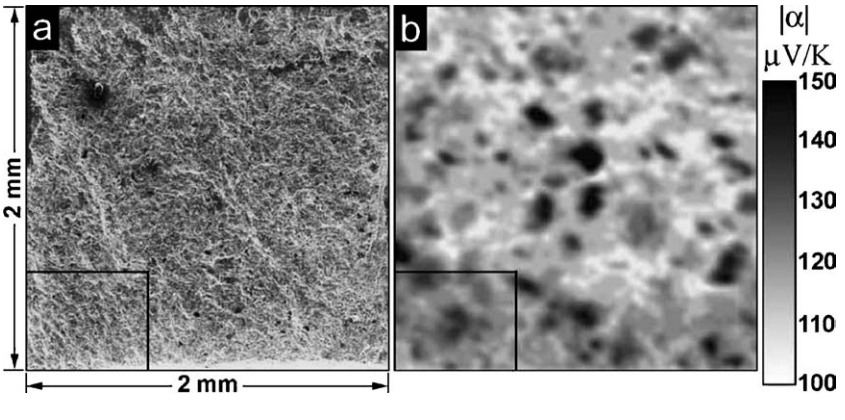


*Figure 5* The morphology (a) and the Seebeck coefficient distribution (b) in the plane vertical to the pressing direction of the hot pressed sample.

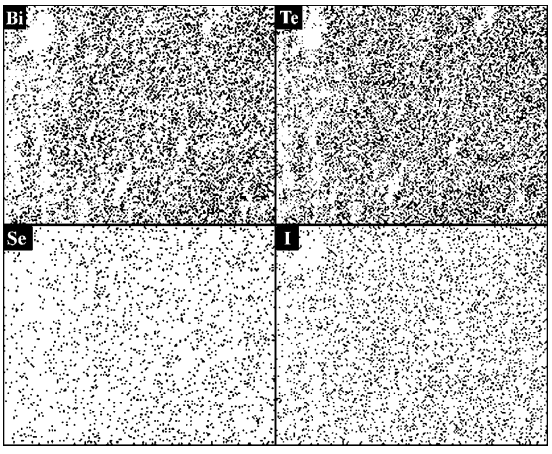


*Figure 6* The element distribution measured by EDS in the left bottom rectangle of Fig. 5.

strongly anisotropic. Although further works should be done to reveal the essence between local Seebeck coefficients and the material intrinsic features, the present work demonstrates that there could be a large difference on local Seebeck coefficients up to 40 $\mu$V/K in a $Bi_2Te_3$ based alloy sample. It is of interest due to the possibility to improve the Seebeck coefficient by the careful control of the fine microstructures of a thermoelectric material. Another significance of the present work is related with the measuring technique of Seebeck coefficients. A large contact area between the measuring probe and the sample is needed to reduce the random errors originated from the variation of the local Seebeck coefficients.

## 4. Conclusion

The microscopic Seebeck coefficient distributions measured in 2 $\times$ 2 mm areas on both zone melted and hot pressed samples of an iodine doped $Bi_2Te_3$ based alloy show a difference of local Seebeck coefficients up to 40 $\mu$V/K. As no remarkable relationship of the local Seebeck coefficients with both surface morphology and chemical composition has been found, crystal defects such as lattice dislocations and stacking faults as well as grain orientations should be the origins of the variation on local Seebeck coefficients. It is suggested therefore that the Seebeck coefficient should be further increased if local fine microstructures of the material could be improved by making them profitable for high Seebeck coefficients.

## Acknowledgments

The work is financially supported by the National Natural Science Foundation of China (50171064), the "863" Program of China (2002AA302406), and the International Bureau of the BMBF of Germany (CHN 01/361).

## References

1. B. C. SALES, *Science* **295** (2002) 1248.
2. F. J. DISALVO, *ibid.* **285** (1999) 703.
3. T. M. TRITT, *ibid.* **283** (1999) 804.
4. B. C. SALES, D. MANDRUS and R. K. WILLIAMS, *ibid.* **272** (1996) 1325.
5. R. VENKATASUBRAMANIAN, E. SIIVOLA, T. COLPITTS and B. O'QUINN, *Nature* **413** (2001) 597.
6. T. C. HARMAN, P. J. TAYLOR, M. P. WALSH and B. E. LAFORGE, *Science* **297** (2002) 2229.
7. D.-Y. CHUNG, T. HOGAN, P. BRAZIS, M. ROCCI-LANE, C. KANNEWURF, M. BASTEA, C. UHER and M. G. KANATZIDIS, *ibid.* **287** (2000) 1024.
8. X. B. ZHAO, X. H. JI, Y. H. ZHANG and B. H. LU, *J. Alloys Comp.* **368** (2004) 349.
9. H.-K. LYEO, A. A. KHAJETOORIANS, L. SHI, K. P. PIPE, R. J. RAM, A. SHAKOURI and C. K. SHIL, *Science* **303** (2004) 816.
10. T. E. SVECHNIKOVA, P. P. KONSTANTINOV, M. K. ZHITINSKAYA, S. A. NEMOV, D. PLATZEK and E. MÜLLER, in Proc. 7th European Workshop on Thermoelectrics (Universidad Pública de Navarra, Pamplona, Spain, 2002.)
11. D. PLATZEK, A. ZUBER, C. STIEWE, G. BÄHR, P. REINSHAUS and E. MÜLLER, in Proc. Int. Conf. on Hermoelectrics, La Grade-Motte, France, 2003, IEEE, Piscataway, NJ 08855, USA, p. 528.

*Received 22 August*
*and accepted 27 September 2004*